

Unambiguous Determination of the Neutrino Mass Hierarchy Using Reactor Neutrinos

Yu-Feng Li, Jun Cao, Yifang Wang, Liang Zhan

Institute of High Energy Physics, Chinese Academy of Sciences, Beijing 100049, China

Abstract

Determination of the neutrino mass hierarchy in a reactor neutrino experiment at the medium baseline is discussed. Observation of the interference effects between the Δm_{31}^2 and Δm_{32}^2 oscillations enables a relative measurement independent of the knowledge of the absolute mass-squared difference. With a 20 kton liquid scintillator detector of the $3\%/\sqrt{E(\text{MeV})}$ energy resolution, the Daya Bay II Experiment at a baseline of ~ 50 km from reactors of total thermal power 36 GW can determine the mass hierarchy at a confidence level of $\Delta\chi_{\text{MH}}^2 \sim (10 \div 12)$ ($3 \div 3.5\sigma$) in 6 years after taking into account the real spatial distribution of reactor cores. We show that the unknown residual energy non-linearity of the liquid scintillator detector has limited impact on the sensitivity due to the self-calibration of small oscillation peaks. Furthermore, an extra increase of $\Delta\chi_{\text{MH}}^2 \simeq 4(9)$ can be obtained, by including the precise measurement of the effective mass-squared difference $\Delta m_{\mu\mu}^2$ of expected relative error 1.5% (1%) from ongoing long-baseline muon neutrino disappearance experiments. The sensitivities from the interference and from absolute measurements can be cross checked. When combining these two, the mass hierarchy can be determined at a confidence level of $\Delta\chi_{\text{MH}}^2 \sim (15 \div 20)$ (4σ) in 6 years.

1 Introduction

An unexpectedly large value of neutrino mixing angle θ_{13} was measured by the Daya Bay Reactor Neutrino Experiment (DYB) [1,2], together with other consistent evidences from the reactor [3,4] and accelerator [5,6] neutrino experiments. It opens a gateway to the measurement of neutrino mass hierarchy (i.e., the sign of Δm_{31}^2 or Δm_{32}^2) and the leptonic CP-violating phase (δ_{CP}). A large value of θ_{13} makes both above measurements easier in the next generation of neutrino oscillation experiments. Possible information on the neutrino mass hierarchy (MH) can be extracted not only from the matter-induced oscillations of long-baseline accelerator neutrino experiments [8–10] and atmospheric neutrino experiments [11,12], but also from the vacuum oscillation in reactor neutrino experiments at medium baseline [13–24].

The MH sensitivity of a future reactor neutrino experiment comes from the interference effect of two separated oscillation modes [16,17] (i.e., two fast oscillations driven by Δm_{31}^2 and Δm_{32}^2). The relative sizes of $|\Delta m_{31}^2|$ and $|\Delta m_{32}^2|$ and the non-maximal value of θ_{12} make it possible to determine the MH in vacuum, immune from the uncertainty of the Earth density profile and ambiguity of the CP-violating phase in atmospheric and long-baseline accelerator neutrino oscillation experiments. Such a measurement is challenging. The energy resolution as the size of $\Delta m_{21}^2/|\Delta m_{31}^2|$ and event number of several tens of thousands are the minimal requirements [17]. Moreover, the spatial distribution of reactor cores [20–22] and non-linearity of the energy response [24] may also degrade the MH sensitivity.

Besides the interference effect in neutrino vacuum oscillations, direct measurements of the flavor-dependent effective mass-squared differences (i.e., Δm_{ee}^2 , $\Delta m_{\mu\mu}^2$ and $\Delta m_{\tau\tau}^2$) [25,26] may also include the MH information. Δm_{ee}^2 from short base-line reactor neutrino experiments (i.e., Daya Bay [27]) and $\Delta m_{\mu\mu}^2$ from the long-baseline accelerator muon-neutrino disappearance are different combinations of Δm_{31}^2 and Δm_{32}^2 . Reactor neutrino experiment at the medium baseline can measure both Δm_{31}^2 (or Δm_{32}^2) and Δm_{21}^2 up to the MH sign. Therefore, a comparison of the effective mass-squared differences in different oscillation scenarios can discriminate the neutrino MH. Considering the MH determination from the Daya Bay II reactor neutrino Experiment, the sensitivity from the interference effect can be improved by including the accurate measurement of the effective mass-squared difference $\Delta m_{\mu\mu}^2$ from accelerator neutrino experiments or Δm_{ee}^2 from reactor neutrino experiments.

Such a study has not been done before and makes sense at least in the following four aspects. (a) we do the first analysis of the non-linearity effect with explicit non-linearity functions; (b) we propose the new idea of non-linearity self-calibration to reduce the non-linearity effect; (c) our strategy to improve the MH sensitivity using the effective neutrino mass-squared differences is different from previous publications; (d) we discuss the effect of baseline differences and provide the real baseline distribution of the approved Daya Bay-II experiment.

The outline of this work is planned as follows. We first give a brief description on the effective mass-squared differences in different oscillation channels in Section 2. Statistical analysis of Daya Bay II is introduced in Section 3. Impact from the energy non-linearity of the liquid scintillator detector is discussed in Section 4. Improved MH sensitivity with the absolute mass-squared difference Δm_{ee}^2 and external $\Delta m_{\mu\mu}^2$ measurements is presented

in Section 5. Finally, we conclude in Section 6.

2 Effective Mass-Squared Differences

In the standard three-neutrino mixing scheme the survival probability for the α -flavor neutrinos is given by [7]

$$P(\nu_\alpha \rightarrow \nu_\alpha) = P(\bar{\nu}_\alpha \rightarrow \bar{\nu}_\alpha) = 1 - 4|U_{\alpha 3}|^2|U_{\alpha 1}|^2 \sin^2 \Delta_{31} - 4|U_{\alpha 3}|^2|U_{\alpha 2}|^2 \sin^2 \Delta_{32} - 4|U_{\alpha 2}|^2|U_{\alpha 1}|^2 \sin^2 \Delta_{21}, \quad (1)$$

where $\Delta_{ij} = \Delta m_{ij}^2 L/4E$, $\Delta m_{ij}^2 = m_i^2 - m_j^2$ and $U_{\alpha i}$ is the element of the leptonic mixing matrix. Note that only two of the three Δ_{ij} are independent because we have the relation $\Delta m_{31}^2 = \Delta m_{32}^2 + \Delta m_{21}^2$ from their definitions.

Strong hierarchy (i.e., $\Delta m_{21}^2 \ll |\Delta m_{31}^2|$) between the magnitudes of Δm_{21}^2 and Δm_{31}^2 (or Δm_{32}^2) is achieved from the analysis of solar (or KamLAND) and atmospheric (or long-baseline accelerator) neutrino oscillation data [28–30]. To separate the fast and slow oscillation modes, we can rewrite the probability in Eq. (1) as

$$P(\nu_\alpha \rightarrow \nu_\alpha) = 1 - 4|U_{\alpha 3}|^2(1 - |U_{\alpha 3}|^2) \sin^2 \Delta_{\alpha\alpha} - 4|U_{\alpha 3}|^2|U_{\alpha 1}|^2 \sin[(1 - \eta_\alpha)\Delta_{21}] \sin[2\Delta_{\alpha\alpha} + (1 - \eta_\alpha)\Delta_{21}] + 4|U_{\alpha 3}|^2|U_{\alpha 2}|^2 \sin[\eta_\alpha\Delta_{21}] \sin[2\Delta_{\alpha\alpha} - \eta_\alpha\Delta_{21}] - 4|U_{\alpha 2}|^2|U_{\alpha 1}|^2 \sin^2 \Delta_{21}, \quad (2)$$

where an effective mass-squared difference is defined as the linear combination of Δm_{31}^2 and Δm_{32}^2 ,

$$\begin{aligned} \Delta m_{\alpha\alpha}^2 &\equiv \eta_\alpha \Delta m_{31}^2 + (1 - \eta_\alpha) \Delta m_{32}^2 \\ &= \Delta m_{32}^2 + \eta_\alpha \Delta m_{21}^2 = \Delta m_{31}^2 - (1 - \eta_\alpha) \Delta m_{21}^2, \end{aligned} \quad (3)$$

and $\Delta_{\alpha\alpha} = \Delta m_{\alpha\alpha}^2 L/4E$. We can choose proper values of η_α to eliminate the terms in the second and third lines of Eq. (2), and therefore keep the independent fast and slow oscillation terms. In general, η_α is not only the function of neutrino mass and mixing parameters, but also the function of the neutrino energy and the baseline.

At the first oscillation maximum of the atmospheric mass-squared difference, we have $\Delta_{21} \ll 1$ and the corresponding oscillation effect is extremely small. Expanding to the linear term of Δ_{21} , we can obtain an effective two-neutrino oscillation scheme, if the parameter η_α satisfies the following relation,

$$\eta_\alpha \simeq \frac{|U_{\alpha 1}|^2}{|U_{\alpha 1}|^2 + |U_{\alpha 2}|^2}. \quad (4)$$

In a neutrino oscillation experiment of this type, such as the short base-line reactor neutrino experiment (i.e., Daya Bay) or the long-baseline accelerator muon-neutrino disappearance experiment, it is impossible to distinguish between the two neutrino mass hierarchies because two degenerate solutions with identical $|\Delta m_{\alpha\alpha}^2|$ but different hierarchies can generate the identical neutrino energy spectrum. The absolute values of Δm_{31}^2

(or Δm_{32}^2) in the two solutions are different due to non-zero Δm_{21}^2 . The value of η_α varies for different oscillation channels due to the flavor-dependent amplitudes in the oscillation probabilities, so the degeneracy of the neutrino MH can be removed by comparing the effective mass-square differences of different neutrino flavors [25, 26].

Using the standard parametrization of the leptonic mixing matrix [7], we get the effective mass-squared differences in Eq. (3) for different channels of neutrino oscillations

$$\Delta m_{ee}^2 \simeq \cos^2 \theta_{12} \Delta m_{31}^2 + \sin^2 \theta_{12} \Delta m_{32}^2, \quad (5)$$

$$\Delta m_{\mu\mu}^2 \simeq \sin^2 \theta_{12} \Delta m_{31}^2 + \cos^2 \theta_{12} \Delta m_{32}^2 + \sin 2\theta_{12} \sin \theta_{13} \tan \theta_{23} \cos \delta \Delta m_{21}^2, \quad (6)$$

$$\Delta m_{\tau\tau}^2 \simeq \sin^2 \theta_{12} \Delta m_{31}^2 + \cos^2 \theta_{12} \Delta m_{32}^2 - \sin 2\theta_{12} \sin \theta_{13} \cot \theta_{23} \cos \delta \Delta m_{21}^2, \quad (7)$$

where terms at the order of $\mathcal{O}(\sin^2 \theta_{13} \Delta m_{21}^2)$ have been neglected for simplicity. We can also calculate the differences of the effective quantities between different flavors as

$$|\Delta m_{ee}^2| - |\Delta m_{\mu\mu}^2| = \pm \Delta m_{21}^2 (\cos 2\theta_{12} - \sin 2\theta_{12} \sin \theta_{13} \tan \theta_{23} \cos \delta), \quad (8)$$

$$|\Delta m_{\mu\mu}^2| - |\Delta m_{\tau\tau}^2| = \pm 2\Delta m_{21}^2 \sin 2\theta_{12} \sin \theta_{13} \csc 2\theta_{23} \cos \delta, \quad (9)$$

where the positive and negative signs correspond to normal and inverted mass hierarchies, respectively.

On the other hand, at the first oscillation maximum of the solar mass-squared difference, such as the reactor neutrino experiment at the medium baseline, we have the approximation of $\sin \Delta_{21} \sim 1$ and $\cos \Delta_{21} \sim 0$. Therefore, we can separate the fast and slow oscillation terms, if η_α fulfills the equation as

$$|U_{\alpha 1}|^2 \cos[\eta_\alpha \Delta_{21}] \cos[2\Delta_{32} + \eta_\alpha \Delta_{21}] + |U_{\alpha 2}|^2 \sin[\eta_\alpha \Delta_{21}] \sin[2\Delta_{32} + \eta_\alpha \Delta_{21}] = 0. \quad (10)$$

One should note that η_α depends on both the neutrino MH and the neutrino energy. The MH sensitivity is encoded in the energy dependence of $\Delta m_{\alpha\alpha}^2$. Moreover, because of the different definitions of $\Delta m_{\alpha\alpha}^2$ in these two oscillation scenarios, the MH sensitivity of the reactor neutrino experiment at the medium baseline can be improved by including the extra measurements of Δm_{ee}^2 in Eq. (5) and $\Delta m_{\mu\mu}^2$ in Eq. (6).

For a reactor neutrino experiment at the medium baseline, corrections to the mass-squared differences from the terrestrial matter effect are around 1% and the induced uncertainties are negligibly small (less than 0.1%). On the other hand, in the muon-neutrino disappearance channel of long-baseline accelerator neutrino experiments, the matter corrections are suppressed by the smallness of θ_{13} and only at the level of 0.2% for the baselines of several hundreds kilometers (e.g., 295 km for T2K [31] and 735 km for NOvA [32]). Moreover, the different signs in the matter potentials of neutrino and antineutrino oscillations are also favorable to increase the discrepancy of different mass-squared differences.

3 Statistical Analysis

The 20 kt liquid scintillator detector of Daya Bay II Experiment [20–22] will be located at equal baselines of 52 km away from two reactor complexes (36 GW in total). In this study we use nominal running time of six years, 300 effective days per year, and a

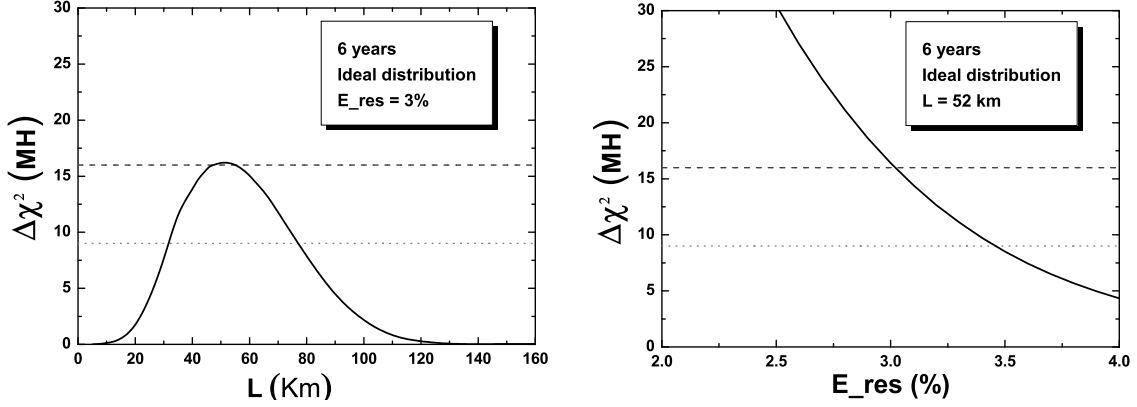


Figure 1: The MH discrimination ability for the proposed reactor neutrino experiment as functions of the baseline (left panel) and the detector energy resolution (right panel) with the method of the least squares function in Eq. (11).

detector energy resolution $3\%/\sqrt{E(\text{MeV})}$ as a benchmark. A normal MH is assumed to be the true one (otherwise mentioned explicitly) while the conclusion won't be changed for the other assumption. The relevant oscillation parameters are taken from the latest global analysis [28] as $\Delta m_{21}^2 = 7.54 \times 10^{-5} \text{eV}^{-2}$, $(\Delta m_{31}^2 + \Delta m_{32}^2)/2 = 2.43 \times 10^{-5} \text{eV}^{-2}$, $\sin^2 \theta_{13} = 0.024$ and $\sin^2 \theta_{12} = 0.307$. The CP-violating phase will be specified when needed. Finally, the reactor antineutrino flux model from Vogel *et al.* [33] is adopted in our simulation¹. Because two of the three mass-squared differences (Δm_{21}^2 , Δm_{31}^2 and Δm_{32}^2) are independent, we choose Δm_{21}^2 and Δm_{ee}^2 defined in Eq. (5) as the free parameters in this work.

To obtain the sensitivity of the proposed experiment, we employ the least squares method and construct a standard χ^2 function as following:

$$\chi_{\text{REA}}^2 = \sum_{i=1}^{N_{\text{bin}}} \frac{[M_i - T_i(1 + \sum_k \alpha_{ik} \epsilon_k)]^2}{M_i} + \sum_k \frac{\epsilon_k^2}{\sigma_k^2}, \quad (11)$$

where M_i is the measured neutrino events in the i -th energy bin, T_i is the predicted reactor antineutrino flux with oscillations, σ_k is the systematic uncertainty, ϵ_k is the corresponding pull parameter, and α_{ik} is the fraction of neutrino event contribution of the k -th pull parameter to the i -th energy bin. The considered systematic uncertainties include the correlated (absolute) reactor uncertainty (2%), the uncorrelated (relative) reactor uncertainty (0.8%), the flux spectrum uncertainty (1%) and the detector-related uncertainty (1%). We use 200 equal-size bins for the incoming neutrino energy between 1.8 MeV and 8.0 MeV.

We can fit both the normal MH and inverted MH with the least squares method and take the difference of the minima as a measurement of the MH sensitivity. The

¹We have tried both the calculated [33] and the new evaluations [34, 35] of the reactor antineutrino fluxes. The discrepancy only influences the measurement of θ_{12} . Both evaluations give consistent results on the MH determination.

Cores	YJ-C1	YJ-C2	YJ-C3	YJ-C4	YJ-C5	YJ-C6
Power (GW)	2.9	2.9	2.9	2.9	2.9	2.9
Baseline(km)	52.75	52.84	52.42	52.51	52.12	52.21
Cores	TS-C1	TS-C2	TS-C3	TS-C4	DYB	HZ
Power (GW)	4.6	4.6	4.6	4.6	17.4	17.4
Baseline(km)	52.76	52.63	52.32	52.20	215	265

Table 1: Summary of the power and baseline distribution for the Yangjiang (YJ) and Taishan (TS) reactor complexes, as well as the remote reactors of Daya Bay (DYB) and Huizhou (HZ).

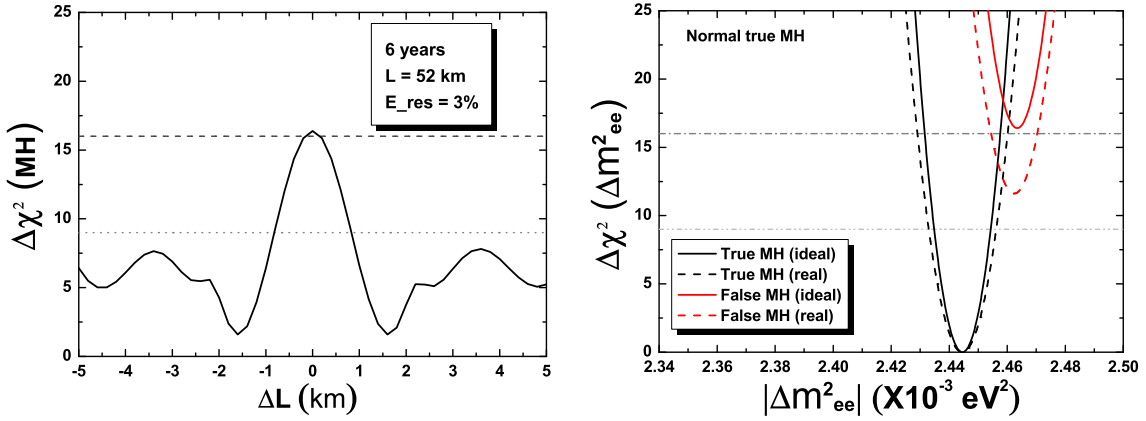


Figure 2: The variation (left panel) of the MH sensitivity as a function of the baseline difference of two reactors and the comparison (right panel) of the MH sensitivity for the ideal and actual distributions of the reactor cores.

discriminator of the neutrino MH can be defined as

$$\Delta\chi_{\text{MH}}^2 = |\chi_{\text{min}}^2(\text{N}) - \chi_{\text{min}}^2(\text{I})|, \quad (12)$$

where the minimization process is implemented for all the relevant oscillation parameters. Note that two local minima for each MH [$\chi_{\text{min}}^2(\text{N})$ and $\chi_{\text{min}}^2(\text{I})$] can be located at different positions of $|\Delta m_{ee}^2|$. This particular discriminator is used to obtain the optimal baseline and to explore the impact of the energy resolution, which are shown in the left and right panels of Figure 1. Ideally a sensitivity of $\Delta\chi_{\text{MH}}^2 \simeq 16$ can be obtained at the baseline around 50 km and with a detector energy resolution of 3%.

The baselines to two reactor complexes should be equal. The impact of unequal baselines is shown in the left panel of Figure 2, by keeping the baseline of one reactor unchanged and varying that of another. A rapid oscillatory behavior is observed and demonstrates the importance of baseline differences for the reactor cores. To evaluate the impact from the spacial distribution of individual cores, we take the actual power and baseline distribution of each core of the Yangjiang (YJ) and Taishan (TS) nuclear power plant, shown in Table 1. The remote reactors in the Daya Bay (DYB) and the possible Huizhou (HZ) power plant are also included. The reduction of sensitivity due to the actual distribution of reactor cores is shown in the right panel of Figure 2, which gives

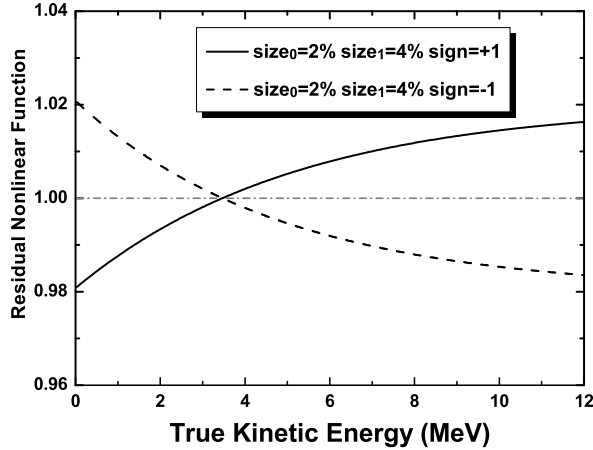


Figure 3: Two classes of typical examples for the residual non-linear functions in our simulation.

a degradation of $\Delta\chi^2_{\text{MH}} \simeq 5$. In all the following studies, the actual spacial distribution of reactor cores for the Daya Bay II Experiment is taken into account.

4 Energy Non-Linearity Effect

The detector energy response is also crucial for Daya Bay II since a precise energy spectrum of reactor neutrinos is required. Assuming the energy non-linearity correction is imperfect, we study its impact to the sensitivity by including in our simulation a residual non-linearity between the measured and expected neutrino spectra. Assume the detector energy non-linearity has the form as

$$\frac{E_{\text{rec}}}{E_{\text{true}}} = \frac{1 + p_0}{1 + p_1 \exp(-p_2 E_{\text{true}})}, \quad (13)$$

where E_{rec} and E_{true} are the reconstructed and true kinematic energy of the positron from the inverse beta decay, respectively. The parameter of p_0 , p_1 and p_2 describe the shape and magnitude of the non-linear functions. We assume that, after the non-linearity correction, the residual non-linearity in measured energy spectrum also has the same function form. The conclusion won't be changed for other residual non-linearity assumptions, because we will use a quadratic function in the predicted spectrum, different from the measured spectrum. We fix $p_2 = 0.2 / \text{MeV}$ and vary p_0 and p_1 as

$$p_0 = \text{sign} \times \text{size}_0 \quad \text{and} \quad p_1 = \text{sign} \times \text{size}_1, \quad (14)$$

where $\text{sign} = \pm 1$ determines the slope, size_0 and size_1 can be a few percent to indicate the magnitudes of the residual non-linearity. Two typical examples with $\text{sign} = \pm 1$ are shown in Figure 3.

By including the residual non-linearity in M_i of Eq. (11), we obtain in Figure 4 updates on the distributions of the $\Delta\chi^2$ function for both true and false neutrino MH, where normal (inverted) MH is assumed to be the true one in upper (lower) panels. Different

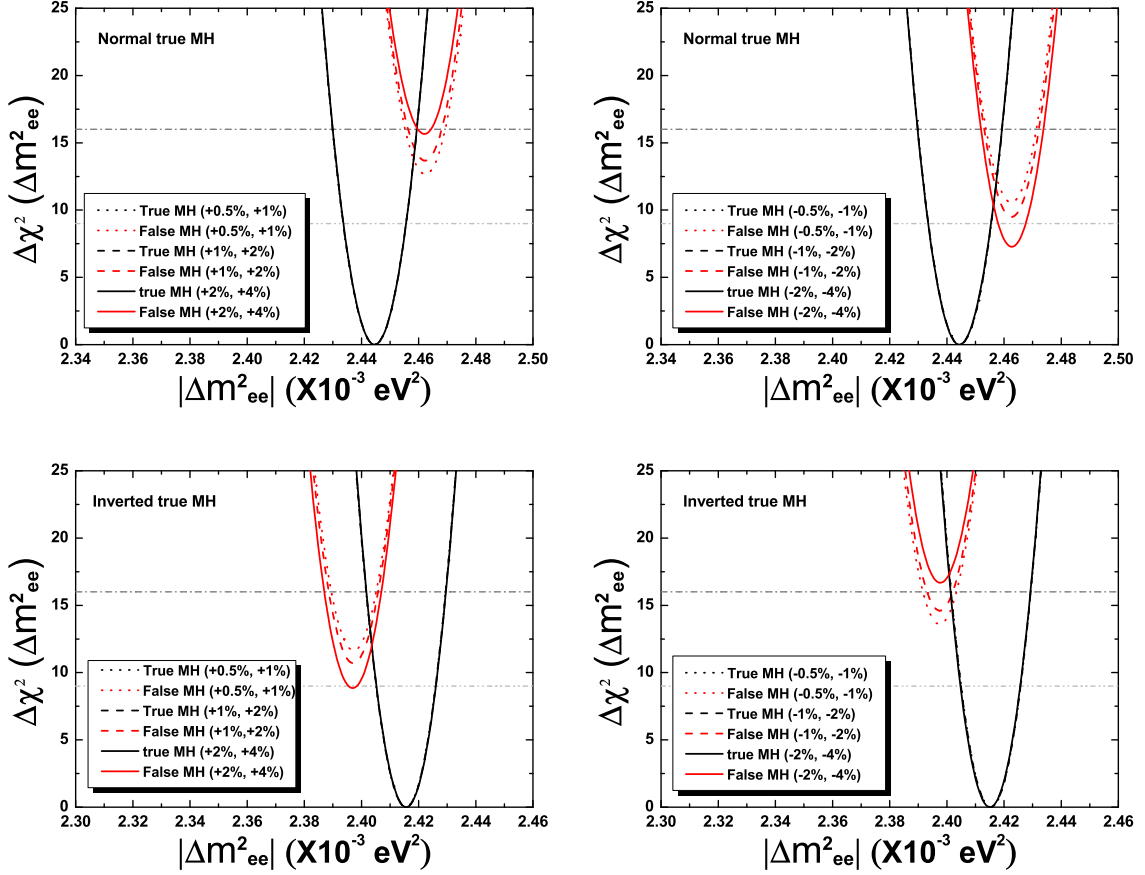


Figure 4: Effects of two classes of energy non-linearity models in the determination of the neutrino MH without the self-calibration in fitting. The normal (inverted) MH is assumed to be the true one in the upper (lower) panels. The sign and size of the non-linear parameters in the form of (p_0, p_1) are indicated in the legend.

classes of the non-linear functions may induce different effects on the MH determination. Comparing to that without non-linearity effects as shown in the right panel of Figure 2, the non-linearity with positive sign (sign = +1) will increase the discrepancy between two neutrino MH scenarios for the normal true MH, but decrease the discrepancy for the inverted true MH. The non-linear functions with negative sign (sign = -1) have opposite effect. Only when the size of non-linearity is as small as 0.5% this effect can be ignored.

For the reactor antineutrino experiment at medium baseline (~ 50 km), we can observe multiple peaks of the Δm_{ee}^2 induced oscillation. Each peak position carries the information of Δm_{ee}^2 . This redundancy can be used to evaluate the energy scale at different energies. Therefore, we can measure to some extent the energy non-linearity by the spectrum itself. We call this effect as the self-calibration of the spectrum. To illustrate, we consider a test quadratic non-linear function in the fitting process,

$$\frac{E_{\text{rec}}}{E_{\text{true}}} \simeq 1 + q_0 + q_1 E_{\text{true}} + q_2 E_{\text{true}}^2, \quad (15)$$

where the central values of three parameters are arbitrary, but the uncertainties are as-

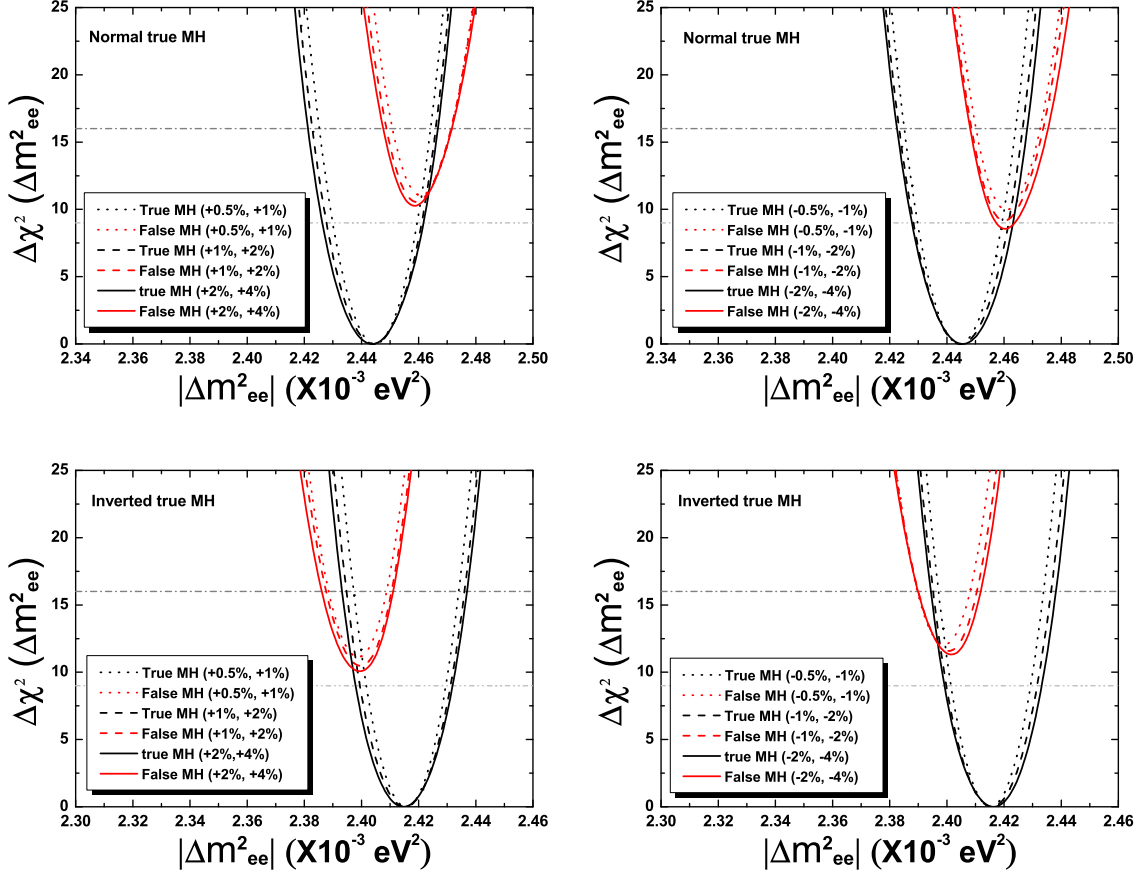


Figure 5: Effects of two classes of energy non-linearity models in the determination of the neutrino MH with the self-calibration in fitting. The normal (inverted) MH is assumed to be the true one in the upper (lower) panels. The sign and size of the non-linear parameters in the form of (p_0, p_1) are indicated in the legend.

sumed to be the same size as the function in Eq. (13). We can define the new least-square function by using the test non-linearity function in T_i and including the corresponding pull terms $\chi_{\text{NL}}^2 = \sum_{i=0}^2 q_i^2 / (\delta q_i)^2$ and derive the MH sensitivity taking into account the non-linearity and self-calibration effects. Considering different sign and size of nonlinearity defined in Eq. (13), we illustrate the $\Delta\chi^2$ function with the self-calibration in fitting in Figure 5, where the normal (inverted) MH is assumed to be the true one in the upper (lower) panels. First we can observe that the degeneracy ambiguity induced by the non-linearity effect can be removed by fitting the parameters of the test non-linearity function and both classes of non-linear functions give the consistent sensitivity of MH determination (see the left and right panels of Figure 4 and 5). Tiny differences can be noticed for different size of the non-linearity because the test quadratic function cannot describe the true residual non-linearity accurately. Second, the width of the $\Delta\chi^2$ functions in Figure 5 is broadened compared to Figure 4. This is because additional uncertainties from the non-linearity parameters are introduced, which can be translated to the uncertainty of the neutrino spectrum and finally to the accuracy of the oscillation parameters.

5 Improvement with External Measurements

Taking into account different definitions of $\Delta m_{\alpha\alpha}^2$ in different oscillation scenarios, precise measurements of Δm_{ee}^2 and $\Delta m_{\mu\mu}^2$ in Eqs. (5) and (6) can provide the additional MH sensitivity in Daya Bay II.

To incorporate the contributions of $\Delta m_{\mu\mu}^2$ from long-baseline accelerator neutrino experiments and Δm_{ee}^2 from short-baseline reactor neutrino experiments, we define the following pull χ^2 function

$$\chi_{\text{pull}}^2 = \frac{(|\Delta m_{\mu\mu}^2| - |\overline{\Delta m_{\mu\mu}^2}|)^2}{\sigma^2(\Delta m_{\mu\mu}^2)} + \frac{(|\Delta m_{ee}^2| - |\overline{\Delta m_{ee}^2}|)^2}{\sigma^2(\Delta m_{ee}^2)}, \quad (16)$$

where $\overline{\Delta m_{\mu\mu}^2}$ ($\overline{\Delta m_{ee}^2}$) and $\sigma(\Delta m_{\mu\mu}^2)$ ($\sigma(\Delta m_{ee}^2)$) are the central value and 1σ uncertainty of the measurement respectively. The combined χ^2 function is defined as

$$\chi_{\text{ALL}}^2 = \chi_{\text{REA}}^2 + \chi_{\text{pull}}^2. \quad (17)$$

As mentioned in the previous Section, we choose Δm_{21}^2 and Δm_{ee}^2 defined in Eq. (5) as the free parameters. The values of $\Delta m_{\mu\mu}^2$ can be calculated by the relations in Eqs. (8) and (9) by assuming different choices of the MH.

In general we need to consider the uncertainties of other oscillation parameters, but the CP-violating phase δ is almost unconstrained and we can absorb the uncertainties of other parameters in that of the phase δ and consider the whole range of CP-violating phase from 0° to 360° . Until 2020, the most accurate measurement of Δm_{ee}^2 may come from the Daya Bay experiment, where an accuracy of 4% [36] can be achieved after a 3-year running of full operation. Numerical analysis demonstrates that the measurement of Δm_{ee}^2 at this level is negligible in the χ^2 function in Eq. (16). Therefore, we focus on the effect of $\Delta m_{\mu\mu}^2$ in this work.

As shown in Eq. (8), because the relative size of Δm_{ee}^2 and $\Delta m_{\mu\mu}^2$ is different for the normal and inverted neutrino MH, the extra pull function χ_{pull}^2 in Eq. (16) can give a

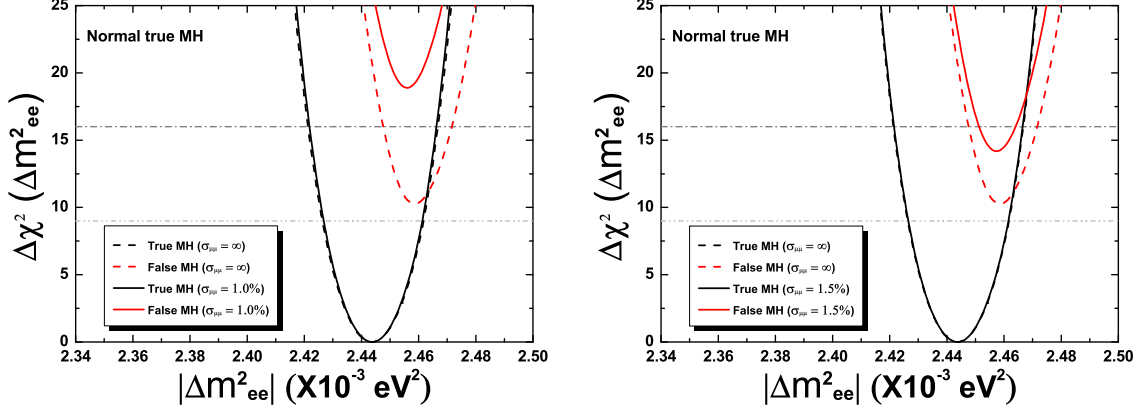


Figure 6: the reactor-only (dashed) and combined (solid) distributions of the $\Delta\chi^2$ function in Eq. (11) and Eq. (17), where a 1% (left panel) or 1.5% (right panel) relative error of $\Delta m_{\mu\mu}^2$ is assumed and the CP-violating phase (δ) is assigned to be $90^\circ/270^\circ$ ($\cos \delta = 0$) for illustration. The black and red lines are for the true (normal) and false (inverted) neutrino MH, respectively. The non-linearity in Eq. (13) is assigned with sign = +1, size₀ = 2% and size₁ = 4%.

non-zero contribution to the discriminator $\Delta\chi_{\text{MH}}^2$ at the magnitude of

$$\chi_{\text{pull}}^2(\text{MH}) \sim \frac{[2 \times \Delta m_{21}^2 (\cos 2\theta_{12} - \sin 2\theta_{12} \sin \theta_{13} \tan \theta_{23} \cos \delta)]^2}{\sigma^2(\Delta m_{\mu\mu}^2)}, \quad (18)$$

and accordingly improve the neutrino MH sensitivity for the reactor neutrino experiment at medium baseline.

To illustrate the effect of the external $\Delta m_{\mu\mu}^2$ measurement, we first fix the non-linearity with sign = +1, size₀ = 2% and size₁ = 4%, choose δ to be $90^\circ/270^\circ$ ($\cos \delta = 0$) and give the separated and combined distributions of the χ^2 functions in Eqs. (11) and (17) in Figure 6, where a 1% (left panel) or 1.5% (right panel) relative error of $\Delta m_{\mu\mu}^2$ is assumed. The black and red lines are for the true (normal) and false (inverted) neutrino MH, respectively. The dashed and solid lines are for the reactor-only [in Eq. (11)] and combined distributions. We can get a value of $\Delta\chi_{\text{MH}}^2 \simeq (10 \div 11)$ for the reactor-only analysis in the least-squares method. As for the contribution from the external $\Delta m_{\mu\mu}^2$ measurement, it is almost negligible if we choose the true MH in the fitting program. However, if the fitting MH is different from the true one, the central value of Δm_{ee}^2 in the χ_{pull}^2 function will change by two units of the difference in Eq. (8), which accordingly results in a significant contribution to the combined χ^2 function. Finally we can achieve $\Delta\chi_{\text{MH}}^2 \simeq 19$ and $\Delta\chi_{\text{MH}}^2 \simeq 14$ for the 1% and 1.5% relative errors of the $\Delta m_{\mu\mu}^2$ measurement.

Next we can discuss the ambiguity of the unknown CP-violating phase δ and evolution of the MH sensitivity with respect to changes of the $\Delta m_{\mu\mu}^2$ error. The $\Delta\chi_{\text{MH}}^2$ dependence on different input errors is shown in Figure 7, where the blue, black and red lines stands for different values of the CP-violating phase ($\delta = 0^\circ$, $\delta = 90^\circ/270^\circ$ and $\delta = 180^\circ$ respectively). In Figure 7, we can notice that the improvement are obvious for an external $\Delta m_{\mu\mu}^2$ measurement better than 2% and becomes significant if we can get to the 1% level. For the effect of the CP-violating phase, it is most favorable for the value close

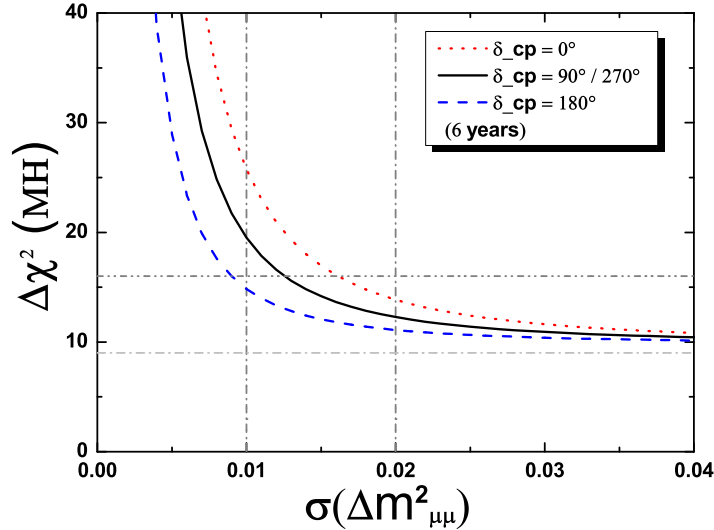


Figure 7: The $\Delta\chi^2_{\text{MH}}$ dependence on different input errors of $\Delta m^2_{\mu\mu}$ is illustrated. The blue dashed, black solid and red dotted lines stands for different CP values ($\delta = 0^\circ$, $\delta = 90^\circ/270^\circ$ and $\delta = 180^\circ$ respectively).

to 180° . The cases of maximal CP violation are in the middle region which are just the cases discussed in Figure 6. The ambiguity of the CP-violating phase can induce an uncertainty of $\Delta\chi^2_{\text{MH}} \simeq 2(4)$ at $\sigma(\Delta m^2_{\mu\mu})/|\Delta m^2_{\mu\mu}| \simeq 1.5\%(1\%)$. The effect of the external $\Delta m^2_{\mu\mu}$ measurement can also be viewed as a probe of the CP-violating phase. If the improvement is much better than the discussion in Figure 6, a preference of δ close to 180° can be achieved. Otherwise, we may get a nearly vanishing CP-violating phase if the situation is totally opposite.

Current best measurement for $\Delta m^2_{\mu\mu}$ from the MINOS experiment [37] gives an error of 4%. Two new experiments T2K [31] and NOvA [32] are in operation or construction and each of them can reach 1.5% by 2020 after finishing of their nominal running plans (5 years of ν mode at 750 kW for T2K and 3 years of ν mode plus 3 years of $\bar{\nu}$ mode at 700 kW for NOvA). If these experiments could extend to another 5-year running, it might be possible to obtain the precision of 1% which will be useful for the measurement of the precision reactor neutrino experiment.

6 Conclusion

In this work, we have discussed the determination of the neutrino MH using the Daya Bay II reactor neutrino experiment at a medium baseline around 50 km away from reactors. Precision measurements of the reactor antineutrino spectrum can probe the interference effect of two fast oscillation modes (i.e., oscillations induced by Δm^2_{31} and Δm^2_{32}) and sensitive to the neutrino MH. The corresponding sensitivity depends strongly on the size of θ_{13} , the energy resolution, the baseline differences and energy response functions. Moreover, the MH sensitivity can be improved by including a measurement of the effective mass-squared difference in the long-baseline muon-neutrino disappearance experiment

due to flavor dependence of the effective mass-squared differences.

We have calculated the MH sensitivity taking into account the real spatial distribution of reactor complexes, and demonstrated that the residual energy non-linearity of the liquid scintillator detector has limited impacts on the sensitivity due to the self-calibration of small oscillation peaks. We numerically calculated the sensitivity by assuming two typical classes of energy non-linearity functions (2%) and discussed the improvement with the external $\Delta m_{\mu\mu}^2$ measurement quantitatively. To conclude, the Daya Bay II Experiment could determine the mass hierarchy unambiguously with a confidence level of $\Delta\chi_{\text{MH}}^2 \sim 14$ (3.7σ) or $\Delta\chi_{\text{MH}}^2 \sim 19$ (4.4σ) in 6 years, for the $\Delta m_{\mu\mu}^2$ uncertainty of 1.5% or 1%.

References

- [1] Daya Bay Collaboration, (F.P. An *et al.*), Phys. Rev. Lett. **108**, 171803 (2012).
- [2] Daya Bay Collaboration, (F.P. An *et al.*), Chin. Phys. C **37**, 011001 (2013).
- [3] Double Chooz Collaboration, (Y. Abe *et al.*), Phys. Rev. Lett. **108**, 131801 (2012).
- [4] RENO Collaboration, (J.K. Ahn *et al.*), Phys. Rev. Lett. **108**, 191802 (2012).
- [5] T2K Collaboration, (K. Abe *et al.*), Phys. Rev. Lett. **107**, 041801 (2011).
- [6] MINOS Collaboration, (P. Adamson *et al.*), Phys. Rev. Lett. **107**, 181802 (2011).
- [7] Particle Data Group, (J. Beringer *et al.*), Phys. Rev. D **86**, 010001 (2012).
- [8] K. Abe *et al.*, (The HyperK Collaboration) arXiv:1109.3262.
- [9] T. Akiri *et al.*, (The LBNE Collaboration) arXiv:1110.6249.
- [10] S. Bertolucci *et al.*, arXiv:1208.0512.
- [11] A. Samanta, Phys. Lett. B **673**, 37 (2009); Phys. Rev.D **81**, 037302 (2010).
- [12] D. J. Koskinen, Mod. Phys. Lett. A **26**, 2899 (2011).
- [13] S.T. Petcov and M. Piai, Phys. Lett. B **533**, 94 (2002).
- [14] S. Choubey, S.T. Petcov and M. Piai, Phys. Rev. D **68**, 113006 (2003).
- [15] J. Learned, S. Dye, S. Pakvasa and R. Svoboda, Phys. Rev. D **78**, 071302 (2008).
- [16] L. Zhan, Y. Wang, J. Cao and L. Wen, Phys. Rev. D **78**, 111103 (2008).
- [17] L. Zhan, Y. Wang, J. Cao and L. Wen, Phys. Rev. D **79**, 073007 (2009).
- [18] P. Ghoshal and S.T. Petcov, JHEP **1103**, 058 (2011).
- [19] S.F. Ge, K. Hagiwara, N. Okamura and Y. Takaesu, arXiv:1210.8141.
- [20] Y.F Wang, talk at ICFA seminar 2008; Neutel 2011, Venice, Italy; NuFact 2012, Williamsburg, VA, USA.

- [21] J. Cao, talk at NeuTel 2009; OCPA 7, Kaohsiung, Taiwan; NuTurn 2012, Gran Sasso, Italy; ICHEP 2012, Melbourne, Australia; NPB 2012, Shen Zhen, China; VCI 2013, Vienna, Austria.
- [22] L. Zhan, talk at NOW 2012, Lecce, Italy; C.G. Yang, talk at Numass 2013, Milano, Italy; Z.M Wang, talk at Nu Geoscience 2013, Takayama, Japan.
- [23] E. Ciuffoli, J. Evslin and X. Zhang, JHEP **12**, 004 (2012).
- [24] X. Qian *et al.*, Phys.Rev. D **87**, 033005 (2013).
- [25] H. Nunokawa, S. Parke and R.Z. Funchal, Phys.Rev. D **72**, 013009 (2005).
- [26] A. de Gouvea, J. Jenkins and B. Kayser, Phys.Rev. D **71**, 113009 (2005).
- [27] Daya Bay Collaboration, (X. Guo *et al.*), arXiv:hep-ex/0701029.
- [28] G.L. Fogli, E. Lisi, A. Marrone, D. Montanino, A. Palazzo and A.M. Rotunno, Phys. Rev. D **86**, 013012 (2012).
- [29] D.V. Forero, M. Tortola and J.W.F. Valle, Phys. Rev. D **86**, 073012 (2012).
- [30] M.C. Gonzalez-Garcia, M. Maltoni, J. Salvado and T. Schwetz, arXiv:1209.3023 [hep-ph].
- [31] Y. Itow *et al.* (T2K), Nucl. Phys. Proc. Suppl. **111**, 146 (2001).
- [32] I. Ambats *et al.* (NOvA) (2004), hep-ex/0503053.
- [33] P. Vogel, G.K. Schenter, F.M. Mann and R. E. Schenter, Phys. Rev. C **24**, 1543 (1981).
- [34] T.A. Mueller *et al.*, Phys. Rev. C **83**, 054615 (2011).
- [35] P. Huber, Phys. Rev. C **84**, 024617 (2011).
- [36] J. Cao, talk at XV International Workshop on Neutrino Telescopes (2013).
- [37] MINOS Collaboration, (P. Adamson *et al.*), Phys. Rev. Lett. **106**, 181801 (2011).